Observation of accelerating Wannier–Stark beams in optically induced photonic lattices

Xinyuan Qi,[1,2] Konstantinos G. Makris,[3] Ramy El-Ganainy,[4] Peng Zhang,[1] Jintao Bai,[2] Demetrios N. Christodoulides,[5] and Zhigang Chen[1,6,*]

[1]Department of Physics and Astronomy, San Francisco State University, San Francisco, California 94132, USA

[2]Department of Physics, Northwest University, Xi'An, Shaanxi 710069, China

[3]Department of Electrical Engineering, Princeton University, Princeton, New Jersey 08544 USA

[4]Department of Physics, Michigan Technological University, Houghton, Michigan 49931, USA

[5]College of Optics—CREOL, University of Central Florida, Orlando, Florida 32816, USA

[6]TEDA Applied Physics Institute and School of Physics, Nankai University, Tianjin 300457, China

*Corresponding author: zhigang@sfsu.edu

Received October 17, 2013; revised December 16, 2013; accepted January 12, 2014; posted January 15, 2014 (Doc. ID 199688); published February 14, 2014

We generate optical beams analogous to the Wannier–Stark states in semiconductor superlattices and observe that the two main lobes of the WS beams self-bend (accelerate) along two opposite trajectories in a uniform one-dimensional photonic lattice. Such self-accelerating features exist only in the presence of the lattice and are not observed in a homogenous medium. Under the action of nonlinearity, however, the beam structure and acceleration cannot be preserved. Our experimental observations are in qualitative agreement with theoretical predictions.

OCIS codes: (350.5500) Propagation; (230.6120) Spatial light modulators; (050.1970) Diffractive optics.
http://dx.doi.org/10.1364/OL.39.001065

Wannier–Stark (WS) ladders and associated electric-field-induced localization predicted and observed in biased semiconductor superlattices have intrigued scientists for decades [1–3]. The concept was subsequently introduced into ultracold atoms with an accelerating optical potential [4] as well as optical periodic structures such as chirped gratings [5] and waveguide arrays superimposed with a linear optical potential [6]. In the latter case of a discrete optical system, stationary eigenfunctions in the form of WS ladders were found.

In recent years, there has been a surge of research interest in the study of Airy beams [7–9], including nonparaxial and nonlinear self-accelerating optical beams [10–16], but much of the work has been carried on in free space or uniform media rather than optical periodic structures. Thus it is natural to ask: can an Airy-like optical beam also self-accelerate in a photonic lattice? Recently, this issue was theoretically investigated, and it was found that WS beams (optical wave packets analogous to WS states in biased semiconductor superlattices) can freely accelerate in uniform waveguide arrays while maintaining their overall intensity profiles during propagation [17]. In particular, the two main lobes of the WS beams self-bend along two opposite hyperbolic trajectories, while there is an asymptotic connection between the WS beams and the Airy beams. Interestingly, such WS beams exist in spite of the fact that the lattice is optically "unbiased," e.g., no linear index inclination (linear potential) is used. This work further stimulated the interest of research in curved beam optics in photonic lattices and photonic crystals [18–21].

In this Letter, we report the first experimental demonstration of self-accelerating WS beams [18]. We show that a WS beam can indeed maintain its shape while its two outer lobes accelerate across a uniform optically induced 1D photonic lattice. However, in the absence of the lattice, the WS beam experiences strong deterioration and can no longer accelerate in the transverse direction. In addition, we find that the symmetric light intensity distribution of a WS beam in uniform lattice will be destroyed under the action of a self-focusing nonlinearity. Our experimental results are in qualitative agreement with theoretical predictions.

In our studies, we first use the discrete model developed in [17] to understand the propagation dynamics of WS beams in optical lattices. Typical numerical simulation results are shown in Fig. 1, where a WS beam is generated by launching a plane wave onto the computer-generated hologram [Fig. 1(a)] coded onto a spatial light modulator (SLM). The hologram is created by interference between a WS beam as obtained in [17] and a tilted plane wave so that the WS beam can be readily retrieved from the first order of the diffraction patterns [22]. When such a WS beam propagates in free space or in a homogeneous medium, it experiences strong linear diffraction and deteriorates as it propagates. However, when it is launched into the 1D waveguide array, the

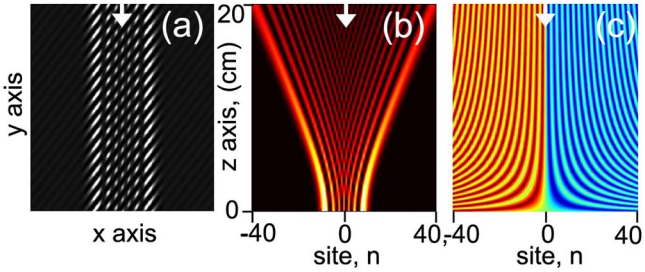

Fig. 1. Numerical simulations of a WS beam in the context of coupled mode theory. (a) Computer-generated hologram on the SLM. (b) Linear propagation of a WS beam through a 1D photonic lattice. (c) The corresponding phase patterns of (b). Site, n marks the waveguide number. (White arrow marks the center of the beam.)

beam maintains its symmetric intensity profile and accelerates in the transverse direction while propagating along the longitudinal z direction [Fig. 1(b)]. Notice that the overall beam width at the output of the lattice is much larger than that at the input. This is due to the self-bending dynamics of the two main lobes of the WS beam along opposite trajectories [14]. On the other hand, the phase of the WS beam propagating in the 1D array oscillates periodically in the transverse direction during propagation along z [Fig. 1(c)], which obeys an antisymmetric function $\theta = n\tan^{-1}(\alpha z)$ as expected from the theory (θ is the phase angle, n is the site number, and α is a constant [17]).

In order to generate and observe the WS beam illustrated in Fig. 1, we perform an experiment with the setup sketched in Fig. 2. A beam from an Argon ion laser (488 nm) is divided into two paths by a polarizing beam splitter. One path (going through the amplitude mask and marked in pink) is for the formation of the 1D photonic lattices in a biased photorefractive crystal using the well-established optical induction method [23]. The other path (going onto the phase only SLM and marked in red) is for retrieving the WS beam from the hologram. The width and the position of the WS beam are carefully adjusted by lenses to match the lattice at the input. The spacing of the lattice is 20 μm, which is about the width of the central lobe of the WS beam at the input. The input and output images are taken by a CCD camera, and their phase profiles are monitored by interfering the WS beam with a tilted broad reference beam (quasi-plane-wave) following the blue path.

Figure 3 depicts the linear experimental results in the 1D optically induced lattice, which is meant to correspond to the theoretical results of Fig. 1. Clearly, there are several major humps (covering 21 waveguides after careful counting) along the transverse direction at the input facet of the crystal, with the intensity maxima located in the two outer peaks distributed somewhat evenly about the central stripe [Fig. 3(a)]. For the cases when the WS beam is launched at normal incidence into the homogeneous crystal without the induced lattice [Fig. 3(b)] and into the uniform 1D waveguide lattice [Fig. 3(c)], the resulting diffraction pattern is dramatically different: without the lattice, its profile is strongly deformed and becomes highly asymmetric [Fig 1(b)], but with the lattice, it expands to about 23 waveguides at the

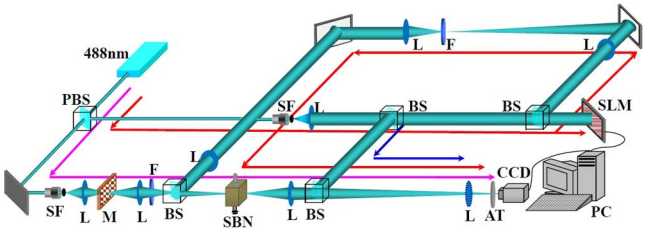

Fig. 2. Schematic of the experimental setup for generation and observation of the WS beam in optically induced lattices. PBS, polarizing beam splitter; SF, spatial filter; M, amplitude mask; F, filter; L, lens; AT, attenuator; SLM, spatial light modulator; SBN, strotium barium niobate crystal. Lines and arrows in pink, red, and blue illustrate the beam paths for the lattice-inducting beam, the WS beam, and the interference reference beam, respectively.

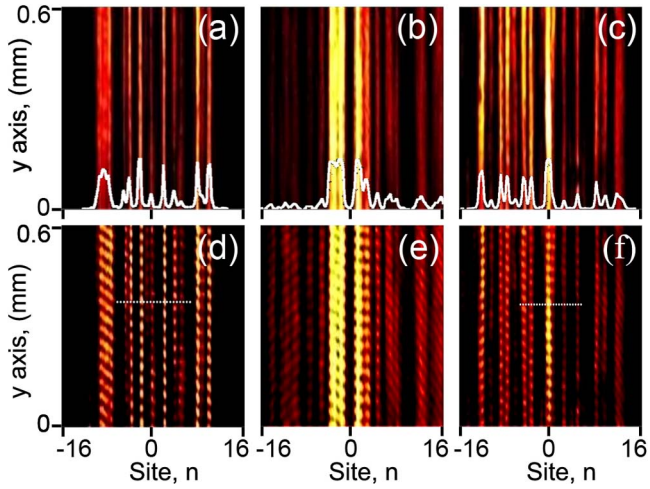

Fig. 3. Experimental results of a WS beam at input (left panels), propagating through a homogeneous medium (middle panels) and through an induced 1D photonic lattice (right panels). Top row shows the transverse intensity patterns; bottom row shows the corresponding interferograms for the phase measurement. (White dotted line serves as a reference line). Site n marks the waveguide number.

output facet while keeping roughly the same profile with most of the energy spreading to both sides [Fig. 3(c)]. The phase structure of the WS beam can be examined from the interferograms as shown in the bottom panels of Fig. 3. The stripes in the transverse direction at the input are almost parallel near central region, indicating that the beam has nearly equiphase at the input. However, from the interferograms taken at the output, one can see that the fringes in the center waveguides interleave each other (thus being out-of-phase), suggesting the phase of the beam on the right and left sides might be antisymmetric about the center stripe. Although the beam has a subtle phase structure, it is important to note that, after propagating through the lattice, the overall WS beam at the output expands slightly when comparing to that at the input, indicating that the two major outer lobes undergo self-acceleration along opposite directions [Fig. 3(c)]. Note that the observed expanding of the WS beam shown in Fig. 3(c) is not as dramatic as that in simulation [Fig. 1(b)], since we are limited by our crystal length (only 1 cm). However, for comparison, a broad Gaussian beam with input size similar to the entire WS beam [as in Fig. 3(a)] would not exhibit appreciable diffraction at this propagation length as does the WS beam [as in Fig. 3(c)]. The bias field used for lattice induction in Fig. 3 is 1.6 kV/cm, and the results are obtained when the WS beam has no nonlinear self-action.

At this point, we want to point out that there are apparent differences between the theoretical results (Fig. 1) and experimental observations (Fig. 3). First, the input intensity pattern [Fig. 3(a)] is not perfectly symmetric with respect to the transverse axis, as compared to those derived from coupled mode theory [Figs. 1(b) and 1(c)]. This asymmetry is more evident in the diffraction pattern of the WS beam [Figs. 3(b) and 3(c)]. The reason for this disagreement is that a WS beam is composed of many higher-order eigenmodes and therefore cannot be described accurately by the discrete model as used for

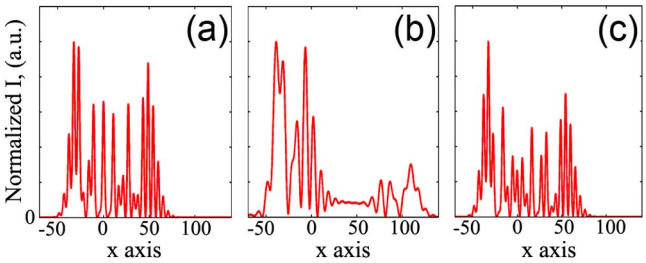

Fig. 4. Theoretical plots of normalized intensity (in a.u.) of a WS beam at (a) input, (b) output after propagating through a homogeneous medium, and (c) output through a 1D photonic lattice.

Fig. 1. For this reason, we also compare our experimental results with simulations based on the continuum model of the paraxial equation of diffraction, which is given in normalized units by $iU_z + U_{xx} + V(x)U + \gamma|U|^2U = 0$, where z is the propagation distance, x the transverse coordinate, U the electric field amplitude, γ the nonlinear Kerr coefficient, and $V(x)$ the optical lattice potential with a period D.

The WS modes are eigenmodes of the form $U(x,z) = \phi(x)\exp(i\beta z)$ of the following linear eigenvalue problem $\gamma = 0$: $\phi_{xx} + [V(x) - ax]\phi = \beta\phi$, where a is the linear tilt of the lattice. We choose the linear tilt in such a way so the WS eigenmodes of the above problem match approximately with the experimental input condition. Then, for this input [Fig. 4(a)], we calculate the linear output of the beam without a lattice [Fig. 4(b)] and with a lattice [Fig. 4(c)]. Clearly, with the lattice present, the WS beam experiences slight expanding [Figs. 4(a) and 4(c)] after careful counting the number of waveguides it covers. Without the lattice, the overall beam diffraction is indeed larger as seen in Figs. 3(b) and 4(b), but the initial beam profile is strongly deformed, and the high intensity region is somewhat localized. Thus better qualitative agreement between experimental and numerical results is obtained with the continuum model. The spatial expansion of the beam and the overall diffraction behavior are very close to that from experiment (Fig. 3). We have to point out that the exact matching between theory and experiment is difficult if not impossible, mainly because in experiments the input WS beam cannot be perfectly coupled to every site of the waveguide lattice.

To further investigate the dynamics of the WS beam, we examine its nonlinear propagation through the photonic lattice. The self-focusing nonlinearity is easily applied under a positive bias field [23], and the strength of the nonlinearity can be fine-tuned by the applied field and/or the intensity of the WS beam. Figure 5 shows the output transverse beam patterns (a) and (b) and corresponding Fourier spectra (d) and (e) at two different levels of nonlinearity (with bias fields 2.0 kV/cm and 2.8 kV/cm, which correspond to nonlinear refractive index changes of about 1.57×10^{-4} and 2.19×10^{-4}, respectively). From Figs. 5(a) and 5(b), one can see that the intensity of the beam shifts more to the left humps and distributes even more asymmetrically with the increased nonlinearity, indicating that the nonlinearity deteriorates the WS beam. We note that this is different from the self-accelerating beams in homogeneous

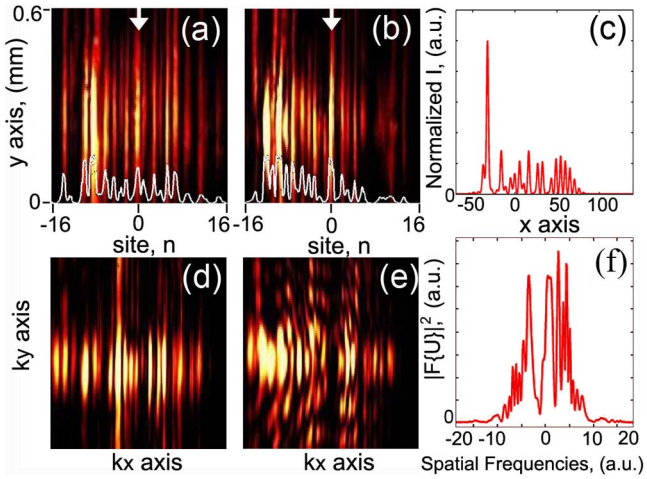

Fig. 5. Experimental results of nonlinear propagation of the WS beam. Shown are output transverse beam patterns after 1 cm propagation distance [(a) and (b)] and corresponding Fourier spectra [(d) and (e)] taken at two different bias fields of 2.0 kV/cm [(a) and (d)] and 2.8 kV/cm [(b) and (e)]. The white arrows mark the center of the beam. k_x and k_y in (d) and (e) are the axes in the momentum space. Theoretical results of output intensity profile and its Fourier spectrum are depicted in (c) and (f), respectively, as obtained from the nonlinear Schrödinger equation (with $\gamma = 1$). Site, n marks the waveguide number.

nonlinear media, where they are not necessarily afflicted by nonlinearity [10–12]. Moreover, the corresponding spectra under different nonlinearities are also measured as shown in Figs. 5(d) and 5(e), suggesting that the Fourier spectra also distribute unevenly and become distorted due to the nonlinear effects. The theoretical results based on the aforementioned nonlinear Schrödinger equation (with $\gamma = 1$) are presented in Figs. 5(c) and 5(f), where the output intensity Fig. 5(c) and the corresponding spectrum Fig. 5(f) are illustrated. We can see that in this case most of the light is shifted to the outermost left lobe, and the strong nonlinearity leads to generation of many new spatial frequencies. Again, the comparison here is meant to be only qualitative; as in our model, the Kerr nonlinearity is employed for simplicity rather than the saturable anisotropic photorefractive nonlinearity, apart from other factors due to complicated experimental situation. Nevertheless, these results illustrate clearly that the propagation of the WS beam is strongly destroyed by the action of nonlinearity. It is worth noting that due to modulation instability, interesting 2D dynamics are observed in Fig. 5 compared to those of Fig. 3. We should also point out that, although our observation suggested that the acceleration of optical beams in nonlinear waveguides leads to beam breakup and instability, there might be stable nonlinear solutions of accelerating beams in optical periodic structures under other conditions yet to be found.

In summary, we have studied both experimentally and theoretically linear and nonlinear propagation of Wannier–Stark beams in 1D uniform photonic lattices. Our results indicate that in the absence of a lattice, a WS beam experiences strong linear diffraction and becomes asymmetrically deformed due to its unique phase and intensity distributions. Yet, in a uniform lattice, a WS

beam maintains its intensity profile and its two lobes "freely" accelerate along two opposite trajectories. Under the action of nonlinearity, however, the profile of the WS beam is destroyed even in the uniform lattice. Our experimental results are in qualitative agreement with numerical simulations. In addition, we have studied the propagation of WS beams in "titled" lattices (straight waveguide arrays but tilted relative to the probe beam direction). We have also found the true diffractionless (no expanding) but accelerating beams in z dependent bending periodic potentials. These results will be reported elsewhere [24]. Our result may bring about new possibilities for studying curved beam optics and self-acceleration in photonic structures.

This work was supported by the AFOSR (MURI FA9550-10-1-0561; FA9550-12-1-0111 and FA9550-13-1-0024) and NSF (PHY-1100842) and by the National Natural Science Foundation of China (11104221), the National Key Basic Research Program of China (2013CB632703).

References

1. J. Bleuse, G. Bastard, and P. Voisin, Phys. Rev. Lett. **60**, 220 (1988).
2. E. E. Mendez, F. Agulló-Rueda, and J. M. Hong, Phys. Rev. Lett. **60**, 2426 (1988).
3. M. Glück, A. R. Kolovsky, and H. J. Korsch, Phys. Rep. **366**, 103 (2002).
4. S. R. Wilkinson, C. F. Bharucha, K. W. Madison, Q. Niu, and M. G. Raizen, Phys. Rev. Lett. **76**, 4512 (1996).
5. C. M. de Sterke, J. N. Bright, P. A. Krug, and T. E. Hammon, Phys. Rev. E **57**, 2365 (1998).
6. U. Peschel, T. Pertsch, and F. Lederer, Opt. Lett. **23**, 1701 (1998).
7. G. A. Siviloglou and D. N. Christodoulides, Opt. Lett. **32**, 979 (2007).
8. G. A. Siviloglou, J. Broky, A. Dogariu, and D. N. Christodoulides, Phys. Rev. Lett. **99**, 213901 (2007).
9. Y. Hu, G. Siviloglou, P. Zhang, N. Efremidis, D. Christodoulides, and Z. Chen, in *Nonlinear Photonics and Novel Optical Phenomena*, Z. Chen and R. Morandotti, eds. (Springer, 2012), Vol. **170**, pp. 1–46.
10. I. Kaminer, M. Segev, and D. N. Christodoulides, Phys. Rev. Lett. **106**, 213903 (2011).
11. A. Lotti, D. Faccio, A. Couairon, D. G. Papazoglou, P. Panagiotopoulos, D. Abdollahpour, and S. Tzortzakis, Phys. Rev. E **84**, 021807 (2011).
12. Y. Hu, S. Huang, P. Zhang, C. Lou, J. Xu, and Z. Chen, Opt. Lett. **35**, 3952 (2010).
13. I. Kaminer, R. Bekenstein, J. Nemirovsky, and M. Segev, Phys. Rev. Lett. **108**, 163901 (2012).
14. F. Courvoisier, A. Mathis, L. Froehly, R. Giust, L. Furfaro, P. A. Lacourt, M. Jacquot, and J. M. Dudley, Opt. Lett. **37**, 1736 (2012).
15. P. Zhang, Y. Hu, D. Cannan, A. Salandrino, T. Li, R. Morandotti, X. Zhang, and Z. Chen, Opt. Lett. **37**, 2820 (2012).
16. I. Kaminer, J. Nemirovsky, and M. Segev, Opt. Express **20**, 18827 (2012).
17. R. El-Ganainy, K. G. Makris, M. A. Miri, D. N. Christodoulides, and Z. Chen, Phys. Rev. A **84**, 023842 (2011).
18. X. Qi, R. El-Ganainy, P. Zang, K. G. Makris, D. N. Christodoulides, and Z. Chen, *CLEO Technical Digest* (Optical Society of America, 2012), paper QM3E.2.
19. K. G. Makris, R. El-Ganainy, X. Qi, Z. Chen, and D. N. Christodoulides, *CLEO Technical Digest* (Optical Society of America, 2012), paper JTu3K.6.
20. I. D. Chremmos and N. K. Efremidis, Phys. Rev. A **85**, 063830 (2012).
21. I. Kaminer, J. Nemirovsky, K. G. Makris, and M. Segev, Opt. Express **21**, 8886 (2013).
22. P. Zhang, S. Huang, Y. Hu, D. Hernandez, and Z. Chen, Opt. Lett. **35**, 3129 (2010).
23. N. K. Efremidis, S. Sears, D. N. Christodoulides, J. W. Fleischer, and M. Segev, Phys. Rev. E **66**, 046602 (2002).
24. K. G. Makris, I. Kaminer, R. El-Ganainy, N. Efremidis, Z. Chen, M. Segev, and D. N. Christodoulides, "Accelerating and diffractionless beams in optical lattices," Opt. Lett. (to be published).